Supporting information

Electronic Structure Modulation of Mo-Doped NiO/Ni Bifunctional Electrocatalyst for Efficient Urea-Assisted Water Splitting

*Shahid Khan [a], Yang Lina [a], Yafei Feng [a], Mingyu Cheng [a], Nazir Ahmad [a] and Genqiang Zhang[a]**

a. Hefei National Research Center for Physical Sciences at the Microscale, CAS Key Laboratory of Materials for Energy Conversion Department of Materials Science and Engineering, University of Science and Technology of China, Hefei, Anhui 230026, P. R. China.

* To whom the corresponding should be referred. gqzhangmse@ustc.edu.cn;

Experimental

Chemicals

In this experiment, all chemicals were used as received without additional purification. Nickel nitrate hexahydrate ($Ni(NO_3)_2 \cdot 6H_2O$, reagent grade 98%), Sodium molybdate ($Na_2MoO_4.2H_2O$, reagent grade 98%) and hydrochloric acid (HCl) were purchased from Aladdin Industrial Corporation. The 5 wt% Nafion solution and potassium hydroxide (KOH, reagent grade 90%) were obtained from Macklin. Furthermore, a commercial Pt/C catalyst (20 wt%) was obtained from Hessen Corporation.

Catalyst Preparation

The Mo-NiO/Ni electrode was synthesized through a simple one-step electrodeposition method. Prior to the deposition, a piece of nickel foam (NF, 1 × 1 cm^2) was thoroughly cleaned several times with 3 M HCl, distilled water, and anhydrous ethanol to remove surface oxides and organic residues. Electrodeposition was carried out at room temperature in a three-electrode setup, using the pretreated NF as the working electrode, a Hg/HgO electrode as the reference electrode, and a graphite rod as the counter electrode. The deposition electrolyte (50 mL) contained 5 mM $Ni(NO_3)_2 \cdot 6H_2O$ and 1 mM $Na_2MoO_4 \cdot 2H_2O$. The process was conducted at -3 V for 20 minutes, and the resulting product was rinsed with water to yield the Mo-NiO/Ni electrode. For comparative purposes, the NiO/Ni electrode was fabricated under the same conditions, except that Na_2MoO_4 was omitted from the electrolyte. Meanwhile, the Pt/C/NF electrode was prepared by dispersing commercial 20% Pt/C powder in a mixture of deionized water, ethanol, and Nafion binder, followed by evenly coating the suspension onto the NF surface. The coated electrode was then dried overnight in a vacuum oven.

Catalyst characterization

The morphology and structure of the products were characterized using field-emission scanning electron microscopy (FESEM, SU-8220, Hitachi), transmission electron microscopy (TEM, HT7700, JEM-2010, Talos F200X, Hitachi), powder X-ray diffractor (XRD, TTR-III, Japan) and Raman spectrometer (Renishaw inVia) with a 532 nm excitation laser. Energy dispersive spectroscopy (EDS) mapping images were collected using a Talos F200X (Thermo Fisher Scientific, USA) transmission electron microscope operating at 200 kV. The surface element and chemical valence of the samples were analyzed using X-ray photoelectron spectroscopy (XPS, ESCALAB 250, UK) with an Al Kα as the excitation source.

Electrochemical measurements

All electrochemical performance of the prepared catalysts were conducted using a three-electrode system with a Corrtest (CS-310X) electrochemical workstation at room temperature. The prepared samples served as working electrode (with a testing area of 0.25 cm^{-2}), while Hg/HgO (1.0 M KOH) and graphite rod were used as the reference and counter electrodes respectively, in alkaline solution. The hydrogen evolution reaction (HER) measurements were carried out in 1.0 M KOH solution, and the Urea oxidation reaction (UOR) measurements were performed in a 1.0 M KOH+0.5 M urea. The polarization curves of the catalysts were recorded using linear sweep voltammetry (LSV) at a scan rate of 5 mV s^{-1}. The Tafel slope was determined by fitting the linear portion of the Tafel plots to the Tafel equation [$\eta = b \log (j) + a$]. Electrochemical impedance spectroscopy (EIS) was performed over a frequency range from 100 kHz to 0.01 Hz with a 10-mV amplitude. The method for calculating the electrochemical active surface area (ECSA) follows the previously reported equation: $ECSA = A_{geo} \times C_{dl} / Cs$, where A_{geo} is the geometric area of the electrode, C_{dl} represents the electric double-layer capacitance of the catalyst in the non-Faradaic region, and C_s is the specific capacitance of the material (typically 0.04 mF cm^{-2}). The double-layer

capacitances (C_{dl}) were obtained using the cyclic voltammograms (CV) method at scan rates of 20-100 mV s^{-1}, the current density differences (Δj = ja - jc) were plotted against scan rates, with the linear slope representing twice the double-layer capacitance (C_{dl}). All potentials measured during the three-electrode performance test were iR-corrected and converted into reversible hydrogen electrode (RHE) scale using the following equation:

$$E_{(RHE)} = E_{(Hg/HgO)} + 0.095 + 0.098 \times pH - 90\% \times iR$$

Computational methods

In this study, theoretical calculations of materials based on the first-principles density functional theory (DFT) were executed utilizing the Vienna Ab initio simulation package (VASP)(1) in conjunction with the Projector Augmented Wave (PAW) methodology.(2) The exchange-correlation functional was managed within the parameters of the Generalized Gradient Approximation (GGA), adopting the Perdew-Burke-Ernzerhof (PBE) functional.(3) The long-range van der Waals interactions are accounted for through the DFT-D_3 approach.(4) We implemented a plane wave basis set with an energy cutoff set at 500 eV, and the geometric relaxation was carried through until the forces acting on each atom were less than 0.05 eV/Å. The sampling of the Brillouin zone was conducted using a 1 × 1 × 1 k-point grid. To assure rigorous consistency, calculations were performed until the energy convergence threshold was less than 10^{-5} eV.

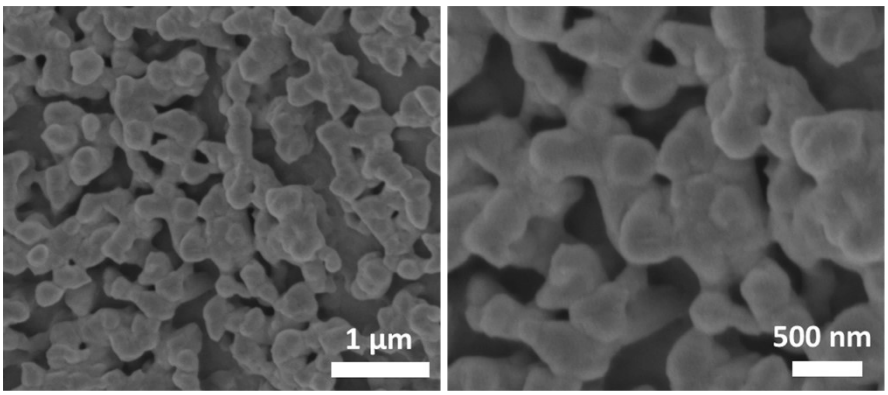

Figure S1. SEM images of NiO/Ni.

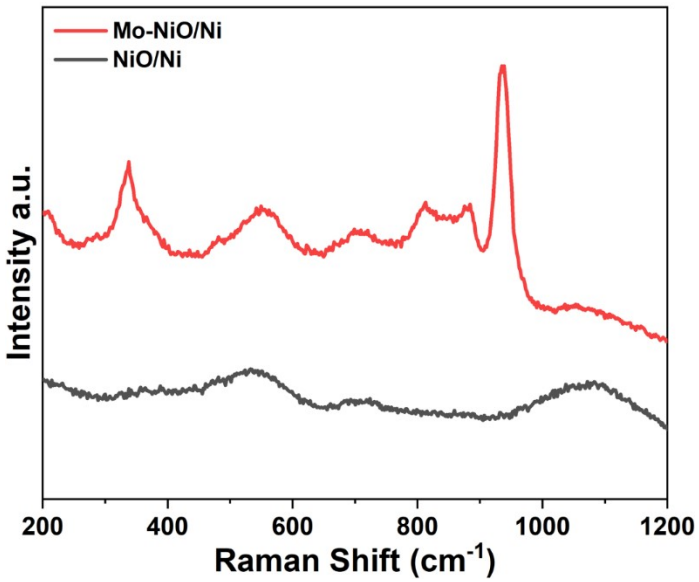

Figure S2. Raman analysis of Mo-NiO/Ni and NiO/Ni.

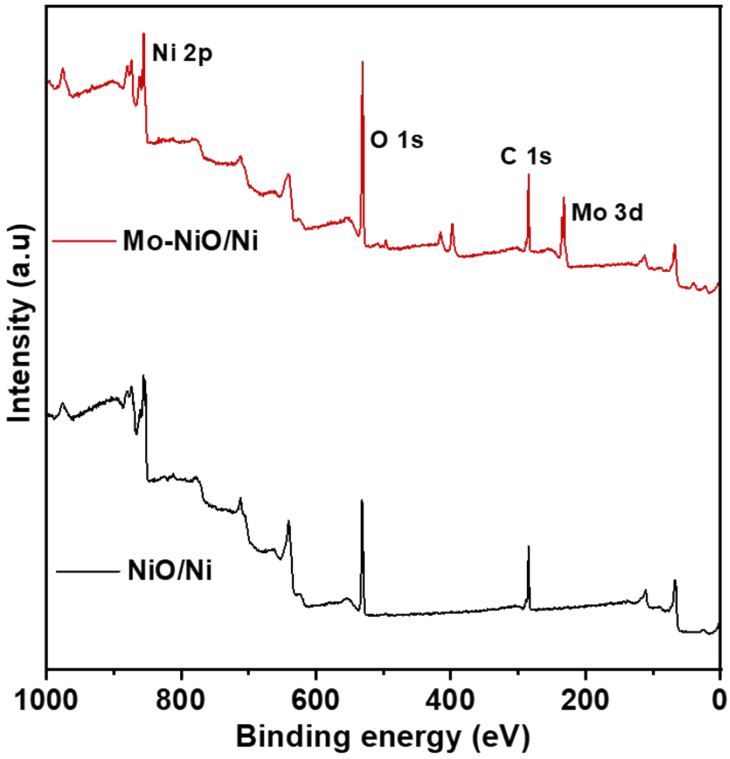

Figure S3. XPS survey spectrum of NiO/Ni and Mo-NiO/Ni

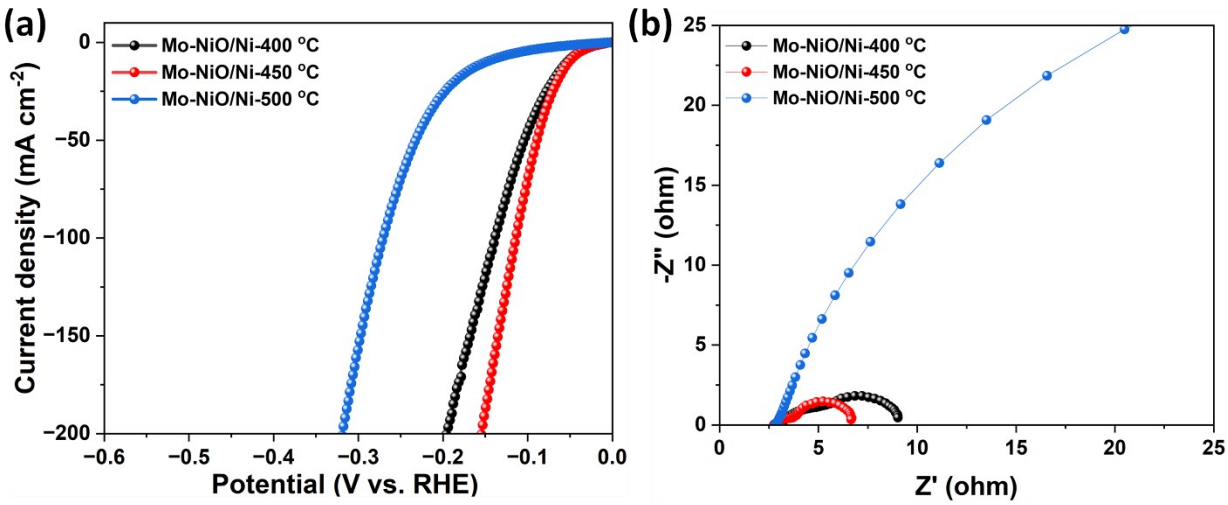

Figure S4. HER of Mo-NiO/Ni annealed at different temperatures in Ar/H_2 atmosphere.

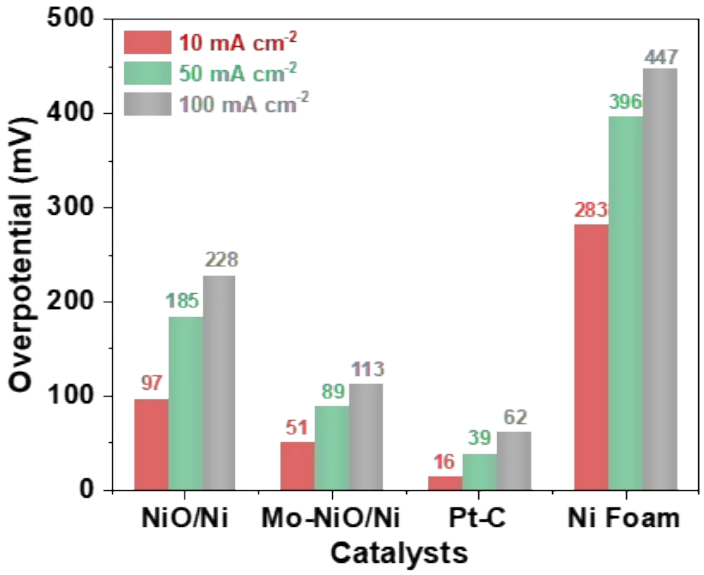

Figure S5. HER overpotential comparison of Mo-NiO/Ni at different current densities

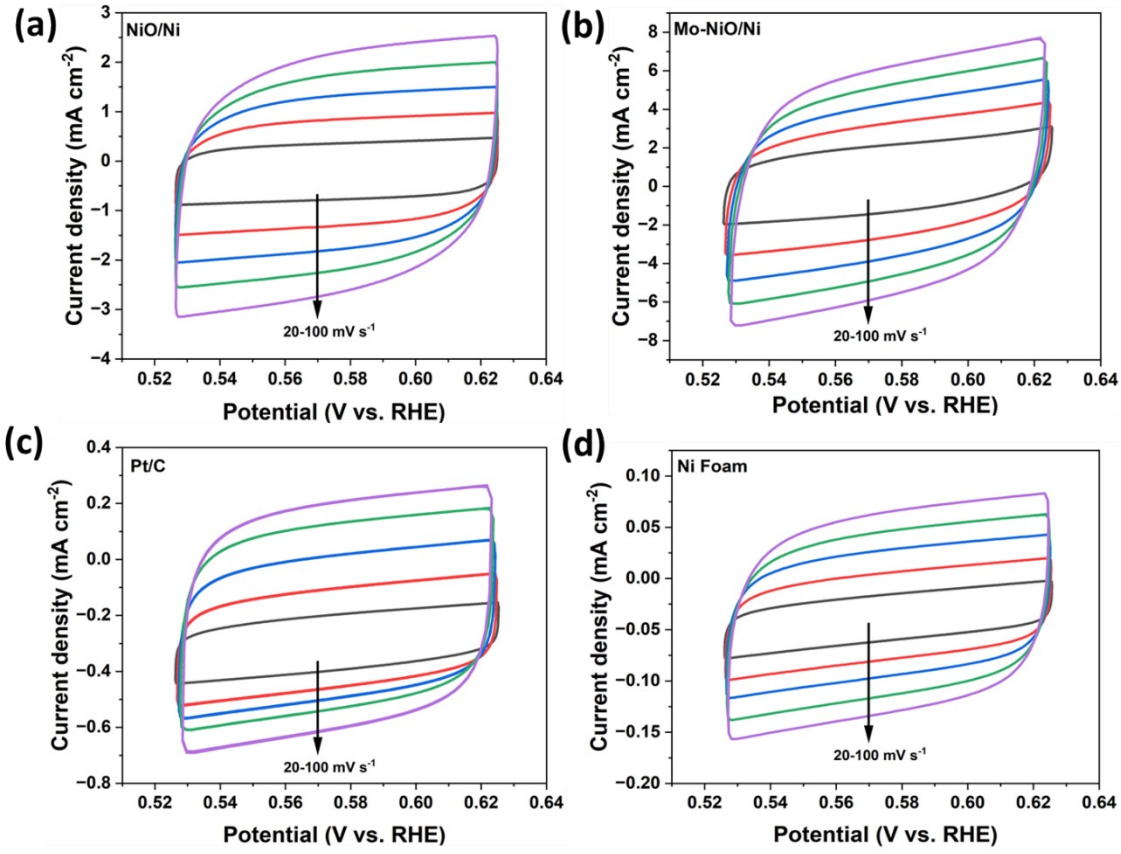

Figure S6. The CV curves of the catalysts measured with the scan rate from 20 to 100 mV s^{-1} in 1.0 M KOH.

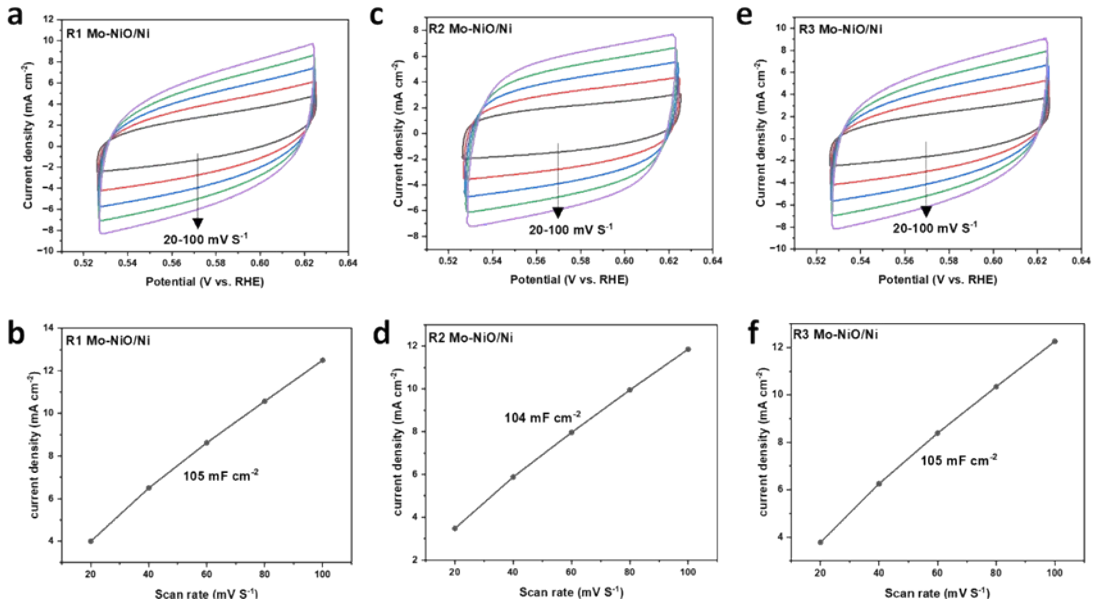

Figure S7. The CV's curves of Mo-NiO/Ni measured with the scan rate from 20 to 100 mV s^{-1} in 1.0 M KOH.

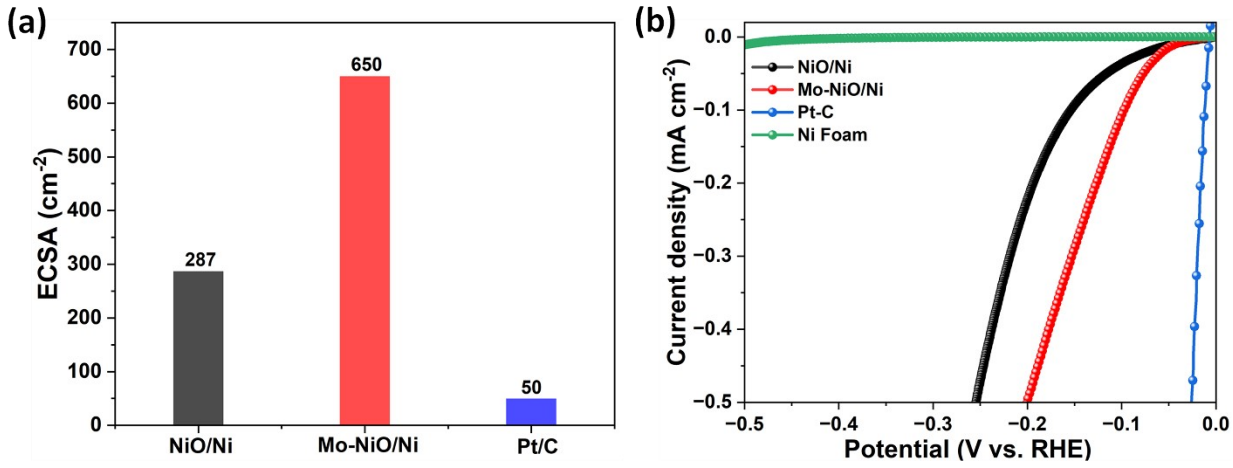

Figure S8. (a) The evaluation of ECSA for different catalysts and (b) corresponding ECSA normalized HER polarization curves.

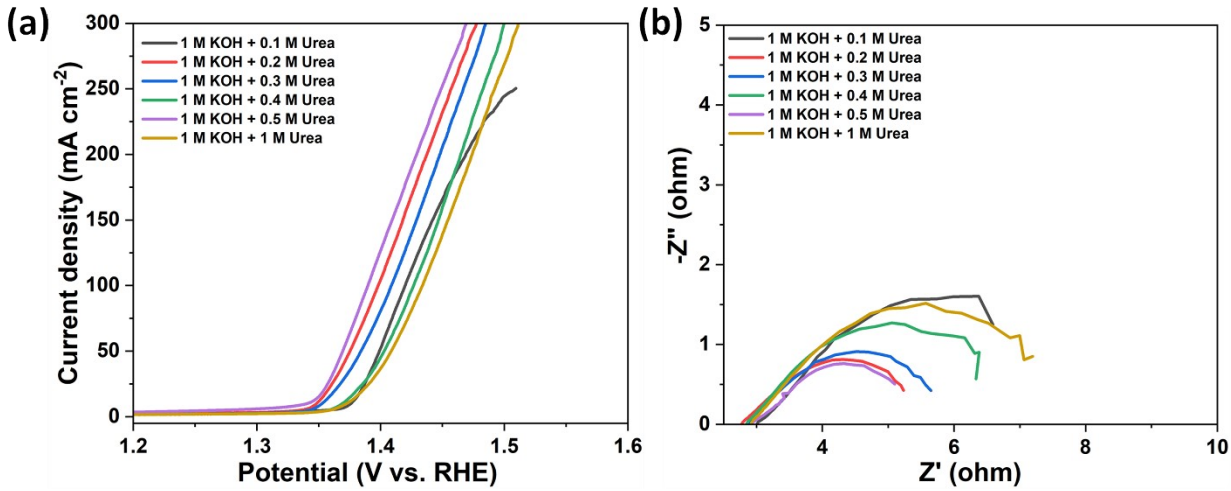

Figure S9. UOR activity of Mo-NiO/Ni tested with varying concentrations of urea with 1 M KOH

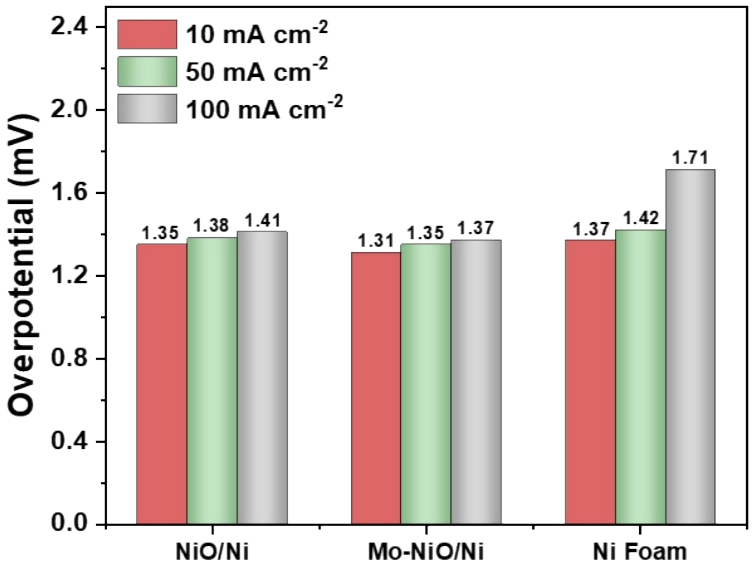

Figure S10. UOR overpotential comparison of Mo-NiO/Ni at different current densities

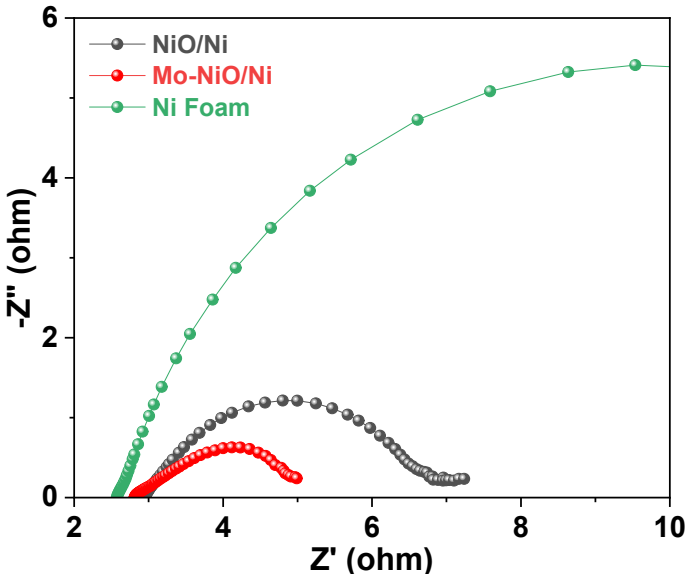

Figure S11. UOR Nyquist plot for UOR of the as-prepared catalysts

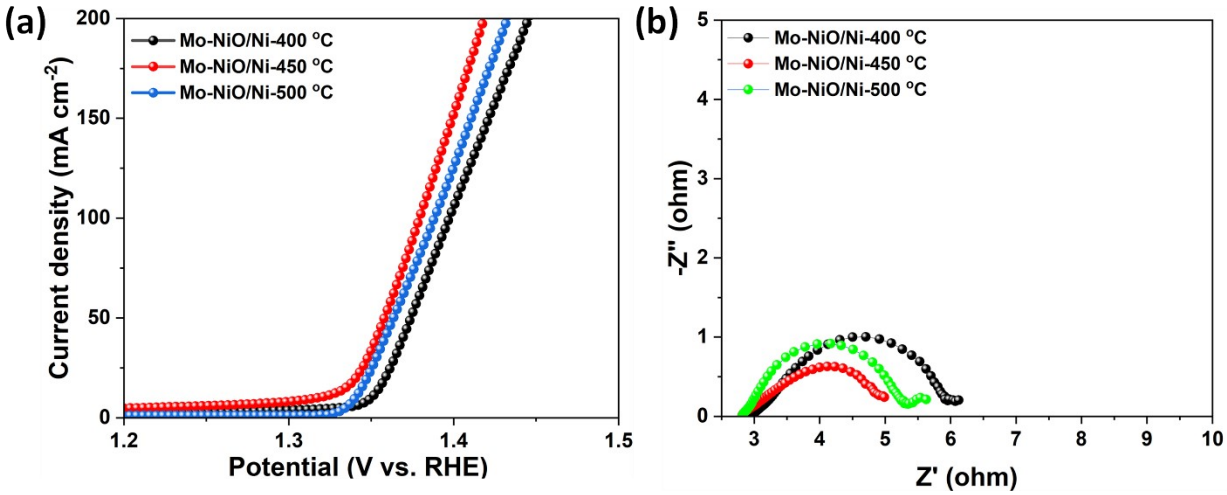

Figure S12. UOR of Mo-NiO/Ni annealed at different temperatures in Ar/H_2 atmosphere.

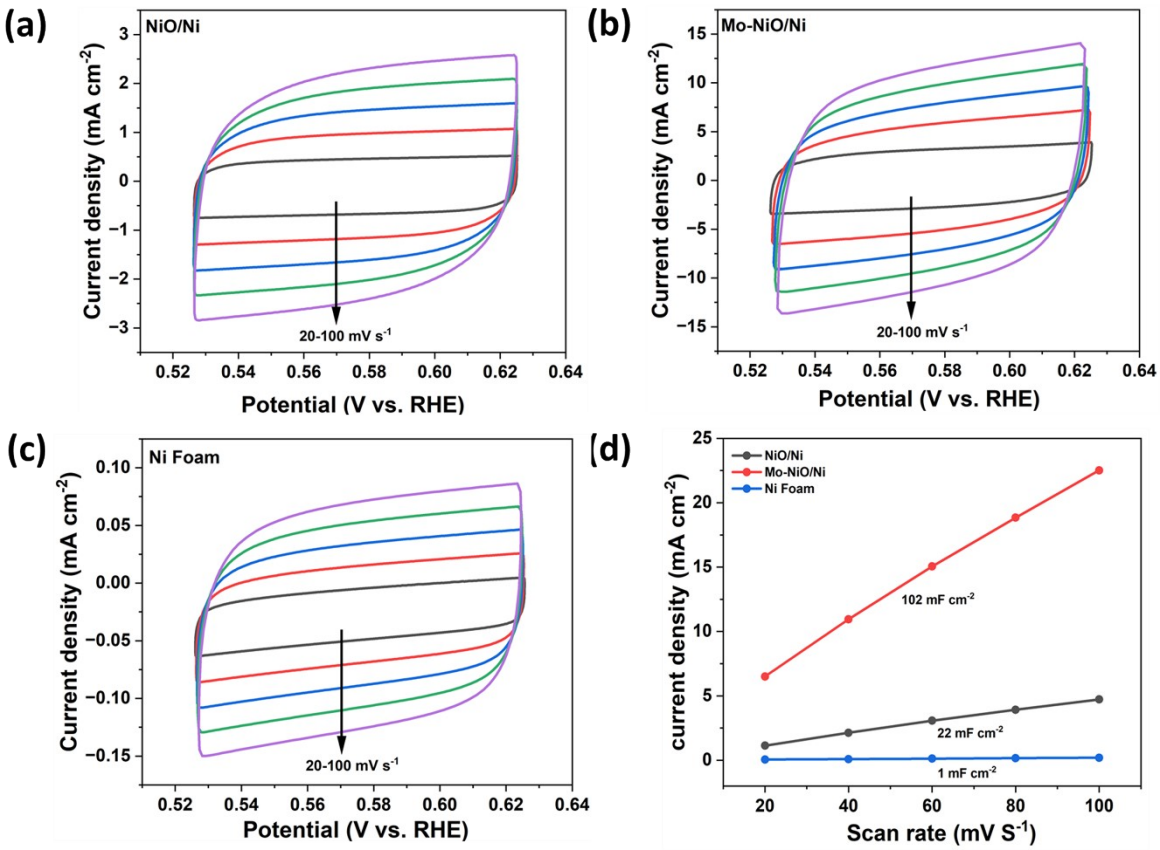

Figure S13. The CV curves and C_{dl} of the catalysts measured with the scan rate from 20-100 mV s^{-1} in 1.0 M KOH+0.5 M urea

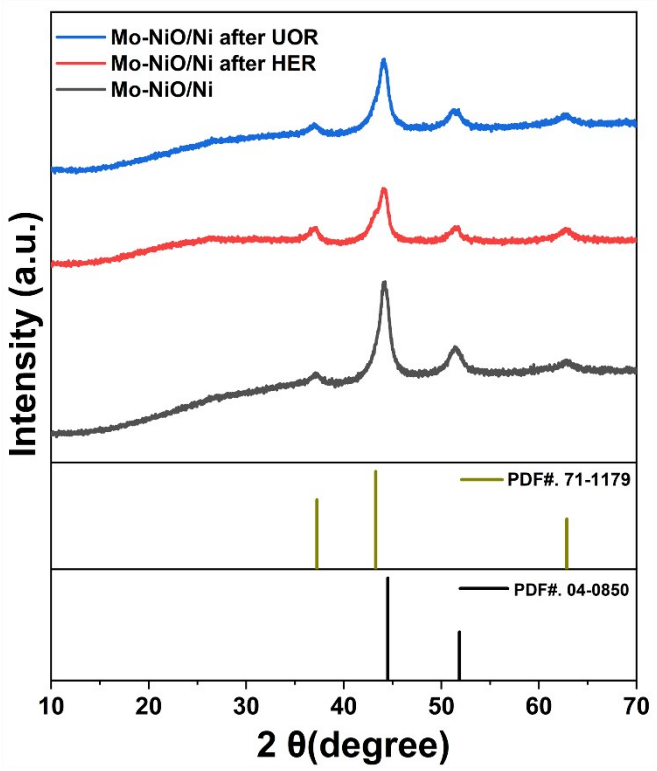

Figure S14. XRD pattern of Mo-NiO/Ni Post-HER and Post-UOR

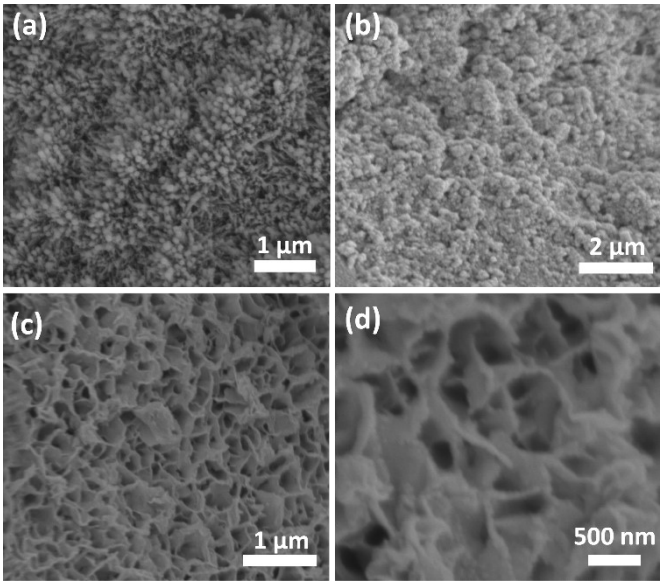

Figure S15. SEM images of Mo-NiO/Ni. (a,b) Post-HER and (c,d) Post-UOR Performance test.

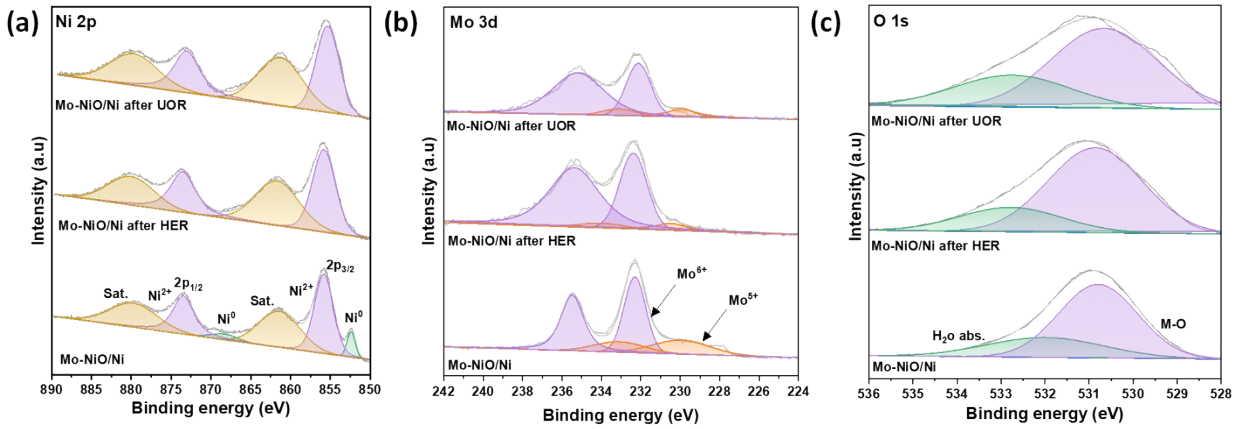

Figure S16. The XPS spectra of Mo-NiO/Ni after HER and UOR test, (a) Ni 2p (b) Mo 3d, and (c) O 1s.

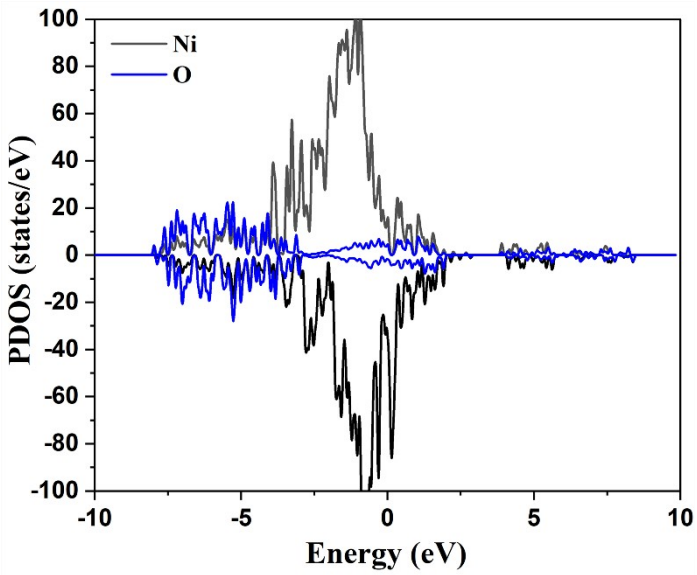

Figure S17. PDOS of NiO/Ni

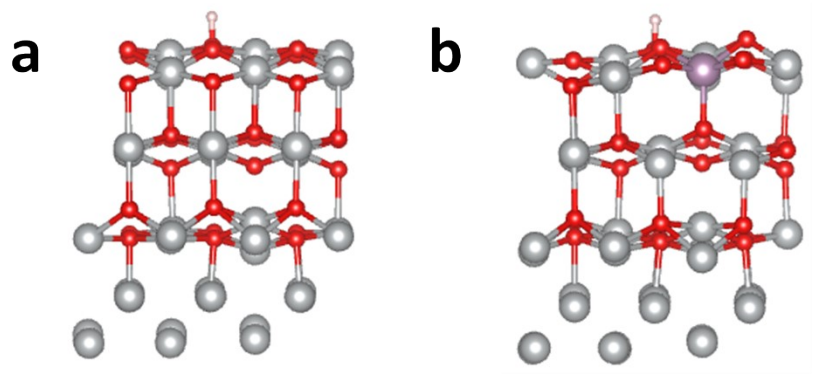

Figure S18. HER structure models of (a) NiO/Ni and (b) Mo-NiO/Ni

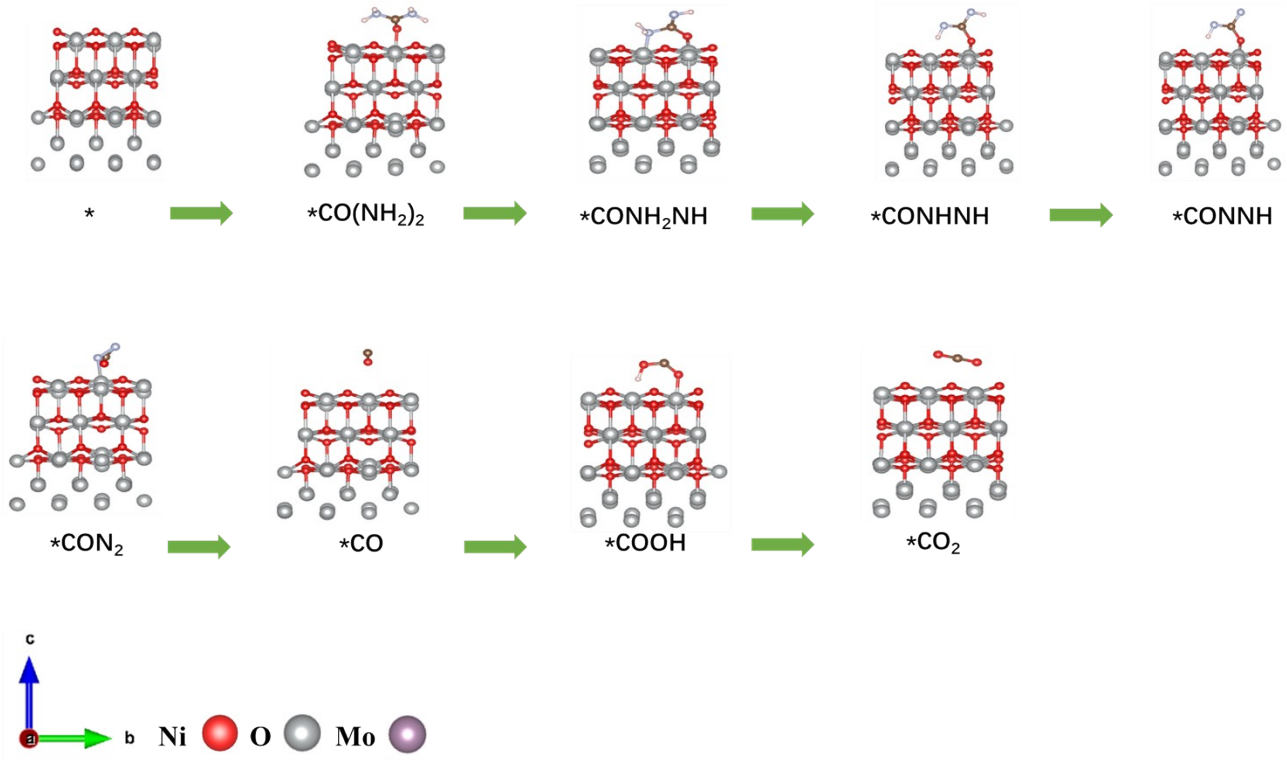

Figure S19. Optimization models for adsorption of different intermediate of $CO(NH_2)_2$ reaction on NiO/Ni.

Table S1. Comparison of HER performance of Mo-NiO/Ni with the reported catalysts in 1.0 M KOH solution

Materials	**Electrolyte**	**η_{10} (mV)**	**Stability duration / mA cm^{-2}**	**Ref.**
Mo-NiO/Ni	**1.0 M KOH**	**51**	**100 h / 100**	**This work**
Bi. NiO	1.0 M KOH	171	100 h / 10	(5)
Ni/NiO-Mo/C@$NiMoO_X$	1.0 M KOH	72	300 h / 10	(6)
Mo-doped Ni/NiO	1.0 M KOH	45	150 h / 10	(7)
NC/NiO-Mo/NF	1.0 M KOH	48	100 h / 50	(8)
NiO/Co_3O_4	1.0 M KOH	110	30 h / 10	(9)
N-Doped NiO	1.0 M KOH	154	10 h / 10	(10)
MoN@NiO	1.0 M KOH	55	100 h / 100	(11)
Ni/NiO/SS	1.0 M KOH	184	12 h / 10	(12)
V-NiO	1.0 M KOH	38	50 h / 100	(13)

Table S2. The comparison of UOR performance between Mo-NiO/Ni and other reported materials.

Materials	Electrolyte	E_{10} (V)	Stability duration / mA cm^{-2}	Ref.
Mo-NiO/Ni	**1.0 M KOH+0.5 M Urea**	**1.31**	**100 h / 100**	**This work**
$Ni_{0.85}Se$/rGO	1.0 M KOH+0.5 M Urea	1.36	6 h / 10	(14)
NiCo-MOF (Ni:Co)	1.0 M KOH+0.5 M Urea	1.32	20 h / 10	(15)
NiCoW	1.0 M KOH+0.5 M Urea	1.28	80 h / 50	(16)
$Ni(OH)_2$/NiO	1.0 M KOH+0.5 M Urea	1.35	50 h / 10	(17)
NiZnCu/NF	1.0 M KOH + 0.5 M Urea	1.33	100 h / 50	(18)
NiMoS/NF	1.0 M KOH+0.5 M Urea	1.33	40 h / 10	(19)
MoO_2-NiO/NF	1.0 M KOH+0.5 M Urea	1.29	100 h / 100	(20)
Ni-$NiMoO_4$/NF	1.0 M KOH+0.5 M Urea	1.32	120 h / 100	(21)
NiCo-MOF/NF	1.0 M KOH+0.5 M Urea	1.32	20 h / 10	(22)

Table S3. Comparison of different catalysts for urea-assisted electrolysis.

Materials	Electrolyte	E_{10} (mV)	Stability duration / mA cm^{-2}	Ref.
Mo-NiO/Ni	**1.0 M KOH+0.5 M Urea**	**1.33**	**100 h / 100**	**This work**
$Ni_{0.85}Se/CoSe_2$	1.0 M KOH+0.5 M Urea	1.29	90 h / 50	(23)
FQD/CoNi-LDH	1.0 M KOH+0.5 M Urea	1.45	100 h / 10	(24)
$N\text{-}Co_9S_8/Ni_3S_2$	1.0 M KOH+0.5 M Urea	1.4	20 h / 20	(25)
NiS/MoS_2	1.0 M KOH+0.5 M Urea	1.46	25 h / 10	(26)
$V\text{-}Co_2P_4O_{12}/CC$	1.0 M KOH + 0.5 M Urea	1.42	20 h / 10	(27)
$Ni\text{-}MOF\text{-}_{0.5}/NF$	1.0 M KOH+0.5 M Urea	1.52	2 h / 10	(28)
$V\text{-}FeNi_3N/Ni_3N$	1.0 M KOH+0.5 M Urea	1.46	25 h / 10	(29)
$NiCo_2S_4NS/CC$	1.0 M KOH+0.5 M Urea	1.49	8 h / 10	(30)

References

1. Kresse G, Furthmüller J. Efficiency of ab-initio total energy calculations for metals and semiconductors using a plane-wave basis set. Computational materials science. 1996;6(1):15-50.
2. Blöchl PE, Jepsen O, Andersen OK. Improved tetrahedron method for Brillouin-zone integrations. Physical Review B. 1994;49(23):16223.
3. Perdew JP, Chevary JA, Vosko SH, Jackson KA, Pederson MR, Singh DJ, et al. Atoms, molecules, solids, and surfaces: Applications of the generalized gradient approximation for exchange and correlation. Physical review B. 1992;46(11):6671.
4. Grimme S, Antony J, Ehrlich S, Krieg H. A consistent and accurate ab initio parametrization of density functional dispersion correction (DFT-D) for the 94 elements H-Pu. The Journal of chemical physics. 2010;132(15).
5. Jo S, Kang B, An S, Jung HB, Kwon J, Oh H, et al. High-Performance Nickel–Bismuth Oxide Electrocatalysts Applicable to Both the HER and OER in Alkaline Water Electrolysis. ACS applied materials & interfaces. 2025;17(8):11946-55.
6. Chen X, Zhu L, Chen H, Tang Y, Lin F, Xie F, et al. Mo-doped Ni/NiO supported on oxygen-deficient NiMoO4 with carbon derived from tannic acid for hydrogen evolution and hydrogen oxidation. Applied Physics Letters. 2025;126(9).
7. Wang Z, Tan X, Wang C, Li G, Yuan S. Mo-doped Ni/NiO as a highly efficient and stable electrocatalyst for the hydrogen evolution reaction. International Journal of Hydrogen Energy. 2025;166:151037.

8. Qiu B, Zhang D, Fang R, Wang Y, Shen B, Dai J, et al. In situ synthesis of Ni, Mo bimetallic crystalline-amorphous co-existing heterostructures for efficient hydrogen evolution reaction. Composites Part B: Engineering. 2025:112956.
9. Huynh N-D, Jana J, Nivetha R, Van Phuc T, Chung JS, Hur SH. 2D siloxene supported NiO/Co3O4 electrocatalyst for the stable and efficient hydrogen evolution reaction. Current Applied Physics. 2022;44:102-9.
10. Wang C, Li Y, Wang X, Tu J. N-doped NiO nanosheet arrays as efficient electrocatalysts for hydrogen evolution reaction. Journal of Electronic Materials. 2021;50(9):5072-80.
11. Feng D, Wang P, Ma B, Zhao X, Chen Y. MoN@ NiO core-shell heterostructure nanorods array for highly efficient electrocatalytic hydrogen evolution reaction. Applied Catalysis B: Environment and Energy. 2025;374:125373.
12. Do HH, Nguyen KB, Nguyen PN, Pham HP. Facile one-step radio frequency magnetron sputtering of Ni/NiO on stainless steel for an efficient electrode for hydrogen evolution reaction. Beilstein Journal of Nanotechnology. 2025;16(1):837-46.
13. Wang S, Li D, Chen D, Liu G, Liang D, Wu J, et al. Controllable modulation of the coordination environment of Ni atoms via vanadium doping to improve the water and hydrogen binding capability of NiO for low-overpotential alkaline hydrogen evolution. Renewable Energy. 2025;240:122227.
14. Zhao L, Chang Y, Jia M, Jia J, Wen Z. Monodisperse Ni0·85Se nanocrystals on rGO for high-performance urea electrooxidation. Journal of Alloys and Compounds. 2021;852:156751.

15. Zhang Q, Kazim FMD, Ma S, Qu K, Li M, Wang Y, et al. Nitrogen dopants in nickel nanoparticles embedded carbon nanotubes promote overall urea oxidation. Applied Catalysis B: Environmental. 2021;280:119436.
16. Liang Z, Yao L, Zhang Y, Li S, Xiao X. 3D NiCoW Metallic Compound Nano-Network Structure Catalytic Material for Urea Oxidation. Nanomaterials. 2024;14(22):1793.
17. Li J, Wang S, Chang J, Feng L. A review of Ni based powder catalyst for urea oxidation in assisting water splitting reaction. Advanced Powder Materials. 2022;1(3):100030.
18. Zhu Q, Li H, Liu S, Zha Q, Ni Y. Flower-like NiZnCu composite microstructures assembled by nanosheets as a highly active bifunctional electrocatalyst for urea-assisted energy-saving hydrogen production. Journal of Materials Chemistry A. 2025;13(48):41855-64.
19. Wang F, Zhang K, Zha Q, Ni Y. Honeycomb-like Ni-Mo-S on Ni foam as superior bifunctional electrocatalyst for hydrogen evolution and urea oxidation. Journal of Alloys and Compounds. 2022;899:163346.
20. Deng Z, Du X, Qian K, Du L, Fang Z, Zhu J, et al. Heterostructured nanoflower-like MoO2–NiO/NF: a bifunctional electrocatalyst for highly efficient urea-assisted water splitting. International Journal of Hydrogen Energy. 2024;62:71-80.
21. Fang C, Li R, Wang X, Duan F, Lin J, Hu Y, et al. Defect-promoted nanoparticles−nanorod Ni−NiMoO4 heterogeneous nanostructures as efficient electrocatalysts to overall water/urea splitting in fresh/sea water. Chemical Engineering Journal. 2024;484:149498.
22. Yao L, Yang Y, Li S, Xiao X. Electronic Structure Regulation Enhances the Urea Oxidation Reaction Performance of the NiCo-MOF Catalyst. Nanoenergy Advances. 2025;5(4):17.

23. Yuan S, Wu Y, Huang L, Zhang Z, Chen W, Wang Y. Engineering Ni0. 85Se/CoSe2 heterojunction for enhanced bifunctional catalysis in urea-assisted hydrogen production. Journal of Colloid and Interface Science. 2025;683:981-94.
24. Feng Y, Wang X, Huang J, Dong P, Ji J, Li J, et al. Decorating CoNi layered double hydroxides nanosheet arrays with fullerene quantum dot anchored on Ni foam for efficient electrocatalytic water splitting and urea electrolysis. Chemical Engineering Journal. 2020;390:124525.
25. Xie H, Feng Y, He X, Zhu Y, Li Z, Liu H, et al. Construction of nitrogen-doped biphasic transition-metal sulfide nanosheet electrode for energy-efficient hydrogen production via urea electrolysis. Small. 2023;19(17):2207425.
26. Gu C, Zhou G, Yang J, Pang H, Zhang M, Zhao Q, et al. NiS/MoS2 Mott-Schottky heterojunction-induced local charge redistribution for high-efficiency urea-assisted energy-saving hydrogen production. Chemical Engineering Journal. 2022;443:136321.
27. Chang XW, Li S, Wang L, Dai L, Wu YP, Wu XQ, et al. Tuning morphology and electronic structure of cobalt metaphosphate via vanadium-doping for efficient water and urea splitting. Advanced Functional Materials. 2024;34(21):2313974.
28. Zheng S, Zheng Y, Xue H, Pang H. Ultrathin nickel terephthalate nanosheet three-dimensional aggregates with disordered layers for highly efficient overall urea electrolysis. Chemical Engineering Journal. 2020;395:125166.
29. Wang J, Sun Y, Qi Y, Wang C. Vanadium-doping and interface engineering for synergistically enhanced electrochemical overall water splitting and urea electrolysis. ACS Applied Materials & Interfaces. 2021;13(48):57392-402.

30. Wang X, Wang J, Sun X, Wei S, Cui L, Yang W, et al. Hierarchical coral-like NiMoS nanohybrids as highly efficient bifunctional electrocatalysts for overall urea electrolysis. Nano Research. 2018;11(2):988-96.